Preprint Cambridge Centre for Computational Chemical Engineering ISSN 1473 – 4273

Sooting tendency of surrogates for the aromatic fractions of diesel and gasoline in a wick-fed diffusion flame

Maria Botero, Sebastian Mosbach, Jethro Akroyd, Markus Kraft [1]

released: 20 January 2014

[1] Department of Chemical Engineering
and Biotechnology
University of Cambridge
New Museums Site
Pembroke Street
Cambridge, CB2 3RA
United Kingdom
E-mail: mk306@cam.ac.uk

Preprint No. 140

Keywords: soot, surrogate fuel, diffusion flame, smoke point, particle size distribution

Edited by
Computational Modelling Group
Department of Chemical Engineering and Biotechnology
University of Cambridge
New Museums Site
Pembroke Street
Cambridge CB2 3RA
United Kingdom

Fax: + 44 (0)1223 334796
E-Mail: c4e@cam.ac.uk
World Wide Web: http://como.cheng.cam.ac.uk/

Abstract

The sooting characteristics of pure aromatic fuels representative of those present in commercial fuels were studied. The experiment involves the non-premixed combustion of the fuel in wick-fed burner. The particle size distributions (PSD) of soot particles were measured at the tip of flames of different heights, using a differential mobility spectrometer (DMS). Substituted aromatics were studied in order to capture the influence of their structure in the final PSD. At the smallest flame height the PSD is bimodal without a strong prevalence of neither the nucleation or coagulation mode, except for trimethylbenze (TMB) that exhibits a large nucleation mode. For larger flame heights the PSD is multimodal, and the coagulation mode enlarges and shifts to larger particle diameters. After the smoke point the PSD presents a single mode of particles with sizes $\sim$ 100nm. Around the smoke point, all fuels show a slight slow down in particle growth probably due to stronger oxidation while the tip is changing from a close defined one to an opened soot trail. Toluene, TMB produced the largest soot particles, tetralin, butylbenzene (BB) and phenylcyclohexane (PCH) the lowest. this evidence indicates that aromatics substituted with larger aliphatics tend to produce smaller soot particles.

1 Introduction

Fossil-derived fuels (gasoline, diesel, jet fuels) are complex mixtures of hundreds of hydrocarbons. The soot particles formed by the combustion of these fuel are widely regarded as pollutants, and are increasingly regulated both in terms of number and mass of particle matter emitted from on road vehicles [29]. This motivates the necessity to study the sooting characteristics of different fuels in terms of their particle sizes and numbers.

Aromatic species in commercial fuels are present in significant amounts [7, 10, 24], and this content can vary between 15-45% by weight depending on the regulations. The most abundant aromatics are 1-ring alkyl-benzenes and 2-ring naphthalenes. Aromatics, being hydrocarbons that contain benzenoid rings, soot much more heavily than other types of hydrocarbons, particularly in non-premixed combustion [12]. They are known to be important contributors to the formation of polycyclic aromatic hydrocarbons (PAHs) which are well-known soot precursors. This may seem obvious given that they do not require the initial creation of a ring, which can be otherwise a rate limiting step in soot formation [11].

Experimentally, one of the targets used to assess the sooting propensity of a fuel is the smoke point (the greatest flame height without smoke emission under laminar diffusion combustion) [3]. A lower smoke point means a higher sooting tendency. The variations in sooting propensity among different fuel types has been explained as the result, mainly, of a dehydrogenation process. The chances of dehydrogenation increase with the stability of the carbon structure, facilitating the removal of hydrogen atoms in comparison with the breaking of carbon bonds [26]. In terms of the smoke point, aromatics are known to have a greater propensity to soot compared to aliphatics [6, 13, 23].

The addition of side chains to aromatic molecules has complex effects. In general increasing the number of side chains increases the sooting tendency, whereas lengthening the chain has the opposite effect [14]. Particularly noticeable is the addition of a methyl branch increasing the sooting propensity. Results of shock tube experiments [9, 19] showed that an increase in the lateral chain size leads to an increase in the soot induction delay (defined as the time interval between the moment at which a fuel is heated by the reflected shock wave and the moment at which soot particles appear) and a decrease in the maximum soot yield, when comparing toluene, n-heptylbenzene and n-butylbenzene.

These results are in agreement with the notion that as the length of the side chain increases, the abstraction of benzylic H atoms will be less important given the large number of alkyl H atoms that can successfully compete [5]. Even though detailed measurements on sooting tendencies of benzene and substituted benzenes [2, 13, 14, 22] have been reported, information on the characteristics of the soot particles that are formed remains scarce.

The purpose of the paper is to study the influence of the structure of some aromatic fuels on the properties of the soot particles formed in diffusion flames. In order to capture the influence of chemical structure, we characterise the soot particles formed in the non-premixed combustion of several hydrocarbons targeted as surrogates for the aromatic fraction of diesel and gasoline fuels. The flow rates and temperature were measured at each flame height, and the soot is characterised using a simple smoke point lamp burner in conjunction with differential mobility spectroscopy (DMS), obtaining information about

the particle size distribution at different flame heights. The fuels were selected based on previous extensive reviews on surrogate fuels [7, 10, 24].

2 Experimental methodology

2.1 Tested fuels

The fuels tested are: toluene, tetrahydronaphthalene (tetralin), phenylcyclohexane (PCH), 1,2,4-trimethylbenzene (TMB) and n-butylbenzene (BB); their chemical structure can be seen in **Figure 1**.

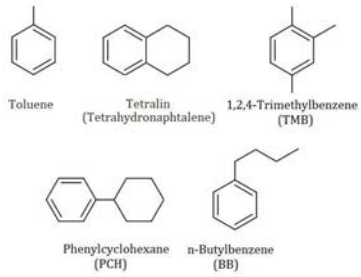

Figure 1: *Chemical structure of tested fuels.*

2.2 Burner and sampling system

In this study, a wick-fed burner that has been previously described (see [30]) was used to generate a laminar diffusion flame of liquid fuel. The burner consists of a cylindrical reservoir, with an inner concentric hole where the wick is placed, and a 7 mm i.d noozle [3]. A light weight threaded Delrin^{TM} fitting was adapted to the outside of the burner tube and connected to the wick sheath. The flame height was able to be adjusted by rotating the threaded fitting and increasing the wick exposure (i.e, increasing the fuel flow rate). At each flame height the fuel flow rate was calculated from the weight loss of the burner, and measured with an analytic balance [30].

The soot particles were sampled using a stainless steel probe with 8 mm inner diameter, enclosed y two water cooling jackets either side of a 0.3 mm sampling hole. The probe was machined such that the sampling hole was at the centre of a flat rectangle, acting as a sampling plate. **Figure 2** depicts the flame sampling system.

At higher soot levels, as per the flames investigated in this work, rapid clogging of the orifice by thermophoretic deposition occurs if the probe is inserted in the flame. Other researchers have encountered the same issues [17, 18], leading to an artificial fall-off of the concentration of particles of sizes below about 10 nm [16]. Due to problems associated with inserting the probe inside the flame, in the present work the soot was sampled only at the tip of the flame (touching the flame at its visible tip).

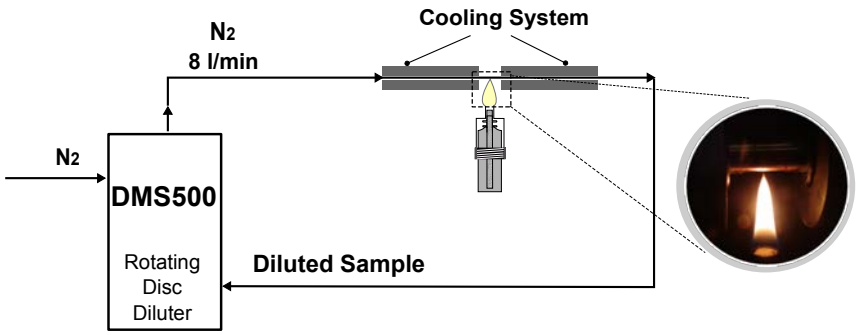

Figure 2: *Sampling system for particle size analysis.*

The sample is drawn into a constant nitrogen dilution flow of approximately 8 litres/min at 0.25 bara resulting in a 30 times dilution of the sample, as well as expansion of the sampled gas avoiding particle agglomeration or coalescence post sampling. A secondary diluter within the particle analyser reduces the particle load on the instrument, using an integral mechanical rotating disc diluter, set to 500 times dilution. Both the first and secondary dilution can be automatically adjusted from the DMS interface.

The total dilution factor is the product of the first and secondary dilutions and is calculated by the DMS, and in this experiments is in the range 10000-15000. Dilution greater than 1000 times was suggested by Siegmann et al. [28] and over 3300 [17] for highly sooting fuels such as gasoline. The diluted sample travels for about 360 ms from the probe orifice to the DMS inlet. Under these experimental conditions diffusive losses to the wall were considered to be negligible by Zhao et al. [32]. The residence time of the gas sample passing through the orifice is calculated to be less than 8 μs before it was diluted with cold nitrogen. This time is sufficiently low to prevent particle losses before dilution. [32]. Similar to previously reported systems [1, 15, 31, 32], independence of the PSD with dilution ratio was achieved at the experimental conditions.

2.3 Soot particle size measurements

The particle analyser used in the present work is a Differential Mobility Spectrometer 500 (DMS) developed and manufactured by Cambustion Ltd. This is a fast particle analyser that enables the PSD to be measured in real-time.

The DMS uses a classifier column operating at 0.25 bara with an external vacuum pump. The sample gas passes through a corona discharge charger, and then flows within a uniform particle-free sheath flow. The particles are deflected towards the rings of a grounded electrometer by the repulsion from a high voltage rod placed in the centre of the cylinder. The landing ring on which a particle is detected depends on its electrical mobility, which is related to the diameter of an equivalent spherical particle; this enables to classify them. The particles transfer their charge to the electrometers amplifier and the resulting currents are translated into particle number and size. The particles are therefore sized based on their mobility diameter, from now onwards referred to as particle diameter.

The soot particles are always sampled at the tip of the flame, and therefore at the centerline, for a series of different flame heights. The flame height was adjusted turning the threaded fitting and sampled again at the tip, this is repeated until the tip of the flame is no longer defined for sampling. Each flame height is sampled for 30 seconds, which corresponds to at least 6 averaged PSDs measured by the DMS. This procedure is repeated at least three times for each fuel.

2.4 Temperature measurements

Centerline temperature measurements were performed with an uncoated 75 μm type R thermocouple (Pt/Pt-13%R), using a rapid insertion procedure to minimise soot deposition [20]. The constant-tension thermocouple design [8] was used as a reference for the set-up. The thermocouple response time was calculated to be $\sim$300 ms. The measured temperature is averaged between 1 and 3 transient times as suggested in the literature [20].

The studied flames are heavily sooting, such that corrections for radiation losses were necessary and were performed as per Shaddix [27] and McEnally et al. [21]. The required values of emissivity were taken from the literature [4]. A Nusselt number of 2 corresponding to a spherical geometry was chosen. This number has been used in similar studies [25].

3 Results and Discussion

Starting from very short flames ($\sim$3 mm), and passing through the smoke point, the flow rate is increased until the tip of the flame is no longer defined, but a trail of soot from the top of the flame. **Figure 3** shows images of different heights BB flames, where each flame was sampled at the visible tip, until a heavy soot trail burst out of the flames as in the last image.

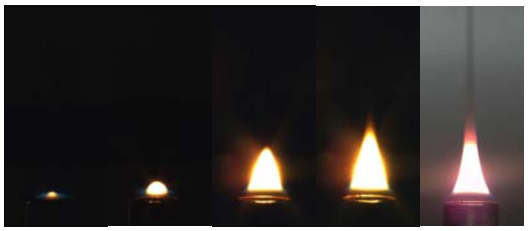

Figure 3: *Images of butylbenzene flames at different flame heights.*

In aromatic fuels the exact smoke point [3] can not be easily determined [30] because flames often display a gradual transition from non-sooting to sooting, and the transition occurs at small flame heights. Tetralin exhibits the smallest value followed by toluene; TMB, PCH and BB had larger smoke points.

3.1 Flow rates and flame tip temperature

The weight loss of the burner containing the liquid fuel was recorded to obtain a continuous measure of the fuel consumption at each flame height. The gradient of the least-squares regression line was used to determine the average fuel uptake rate. Excellent linearity was obtained, giving evidence of a constant flow rate at a given flame height. This result is consistent with a previous investigation [30] testing toluene and PCH.

Figure 4 presents the results of the fuel uptake rate as a function of flame height for all the studied fuels. The data shows that all the fuels obey the same linear relationship within experimental error. The largest differences were 17% and are mainly observed between PCH and BB, but in most of the cases it was below 10%. These results indicate that a given flow rate of fuel will produce a flame of the same height independent of the fuels considered in this work, such that it is possible to compare flames burning different fuels at the same height.

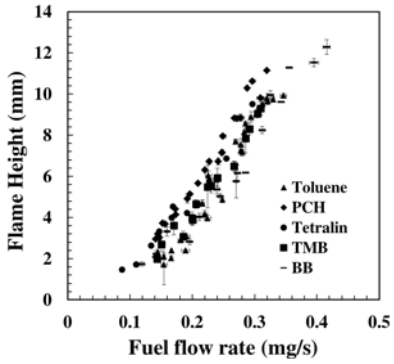

Figure 4: *Mass flow rates at each flame height for all studied fuels*

Results of the temperature at the sampling point (tip of the flame) are shown in **Figure 5**. As the flame height (i.e. flow rate) increases, the temperature at the tip decreases. All the fuels have similar temperatures, except tetralin which consistently presents lower temperatures, where the gap can be as large as $\sim$140 K.

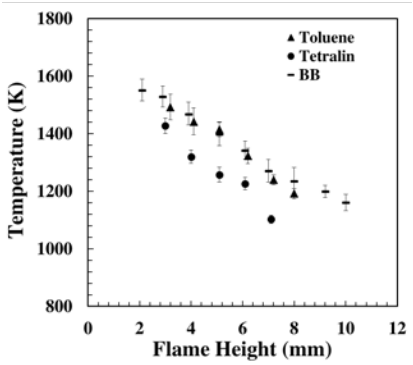

Figure 5: *Temperature at the tip of different flame heights for all tested fuels*

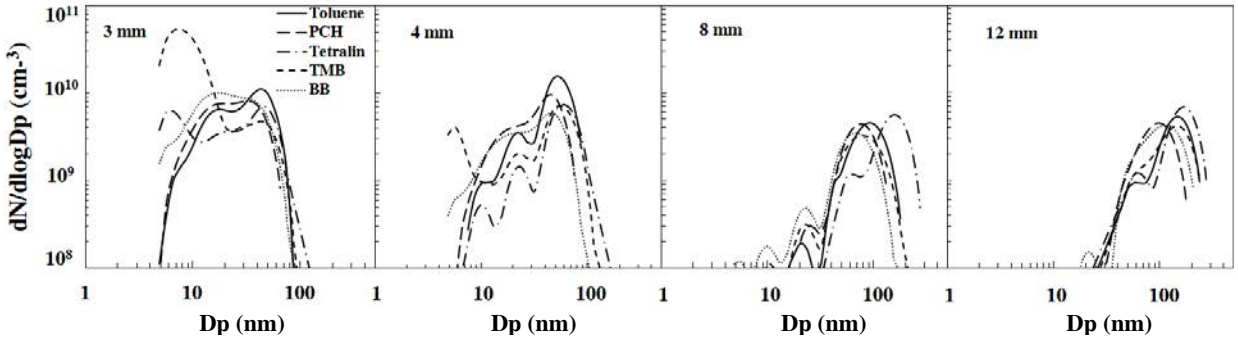

Figure 6: *PSDs for aromatics at different flame heights.*

3.2 Particle size distributions

The particle size distribution as a function of flame height for different aromatics is presented in **Figure 6**. At a very low heights of 3 mm, the yellow luminosity that characterises the presence of soot is observed at the tip of the flame (see **Figure 3**), while the annulus looks bluish. The PSDs consists of two modes: one at lower particle sizes ($\leq$ 15 nm) of mainly primary particles created by the inception process; and a second mode of larger agglomerates (around 40 nm). TMB exhibits significantly more particles in the nucleation mode compared to the other fuels.

At a flame height of 4 mm multiple modes are observed, with predominance of an agglomeration mode of large particles (shifting the PSD to the right, to larger diameters). At 8 mm flame height, the PSD is composed of one large accumulation mode. It can be observed that tetralin has significantly larger soot particles. It is worth noticing that this fuel has the lowest smoke point ($\sim$6.5 mm), which means that at this flame height (and sampling at the tip) soot has broken through the flame tip. For larger flame heights (12 mm), beyond the smoke point of all the fuels, the PSD shifts to diameters larger than 100 nm. BB and PCH, having the largest smoke points ($\sim$8.5 mm), exhibit smaller shifts to large particle sizes.

Figure 7 shows the total number of particles (N) and particle mean diameter ($\langle dp \rangle$) as a function of flame height for each aromatic fuel. At small flame heights N is large for all the fuels, indicating the formation of many primary particles. The large number of young soot particles causes intense coagulation and leads to a decrease of N. As flame height increases, beyond $\sim$7 mm the number of particles stabilises and remains fairly constant. The largest flames sampled exhibit a slight increase in N, which may be a consequence of a decrease in oxidation as observed by the soot trail.

The $\langle dp \rangle$ (**Figure 7**) exhibits a continuous growth. At small heights the particles detected had sizes around 20 nm and grow quickly due to coagulation as suggested by the reduction in N. Three zones with different slopes are observed in the evolution of $\langle dp \rangle$. Initially $\langle dp \rangle$ grows at a certain rate (at flame heights below 6 mm), but as the flame height approaches the smoke point (between 6.5 and 9 mm for these fuels), this rate slows down. After the smoke point region (above 9 mm flame height), $\langle dp \rangle$ grows again at a higher rate. As the flame passes through the smoke point its shape changes from a round well defined tip, to a blurry elongated tip with a visible soot trail (this transition can be observed in **Figure 3**).

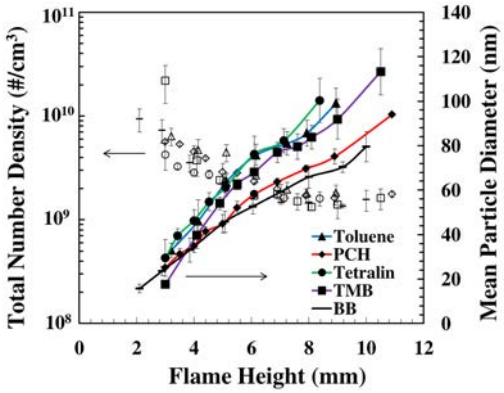

Figure 7: *Mean soot particle diameter and number of particles as a function of flame height.*

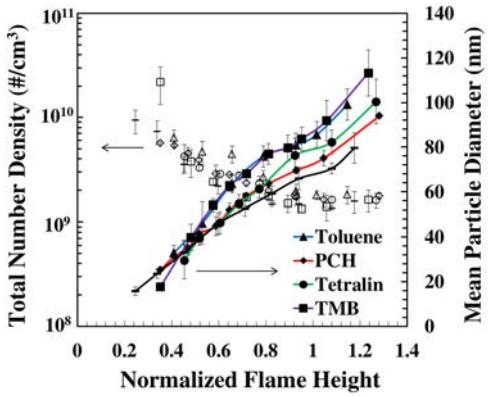

Figure 8: *Mean soot particle diameter and number of particles as a function of flame height normalised by the smoke point*

This entails that in this transition stage, soot sampled from the tip is passing through the flame front and being oxidised, but this oxidation is not complete. After the smoke point, the soot trail breaks the flame tip, opening the flame and allowing the particles to leave, such that the size of $\langle dp \rangle$ increases again. With this evidence and within the experimental error, the fuels can be gathered in two groups. Toluene, tetralin and TMB, which produce the largest particles and PCH and BB which produce relatively smaller particles.

It is important to note that when comparing fuels at the same flame height we are approximately comparing particles with the same residence time (given that the flowrates are similar). However, at the same flame height some fuels can be below the smoke point, while others can be already emitting soot particles. For example at 8 mm flame height tetralin is emitting particles, whilst toluene is in the transition stage, but the other fuels are still below their smoke point. In order to investigate in greater detail the trends below and above the smoke point **Figure 8** presents N and $\langle dp \rangle$ as a function of flame height normalised by the smoke point.

Values of normalised flame height below 1 correspond to flames below the smoke point. Values greater than 1 correspond to a smoking flame. As mentioned before, the change from non-emitting to smoking flame of aromatic fuels is gradual, therefore the smoke

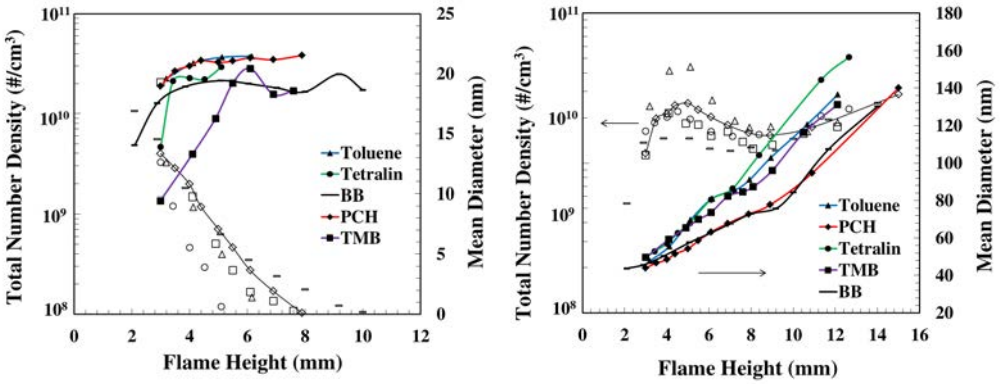

(a) *First mode of small particles* **(b)** *Second mode of large particles*

Figure 9: *Mean soot particle diameter and number of particles as a function of flame height*

point is not precise but a range (around the value of 1 in **Figure 8**). Below the smoke point toluene and TMB exhibit a similar increase in particle size, while tetralin, PCH and BB show a slower increase. After the smoke point the tendencies remain similar but tetralin achieves larger particles and locates in-between the two groups of fuels, although within the experimental error it could fall in any of the two groups.

Given that the PSD for all fuels showed a multimodal behaviour for most of the studied flame heights, the change of N and $\langle dp \rangle$ as a function of flame height for the two main modes was investigated and is depicted in figures **Figures 9a** and **9b** respectively. In the first mode ($dp \leq 31$ nm) the particle size is small at low flame heights and increases rapidly to a constant value around 20 nm for all fuels. This size correspond to incepted particles that have experience some growth by surface reactions and coagulation. TMB exhibit the lowest values of $\langle dp \rangle$ at the smaller flame heights. The steep decrease in N with increasing flame height indicates that coagulation processes occur at fast rates contributing to the formation of larger particles.

The accumulation mode (**Figure 9b**) represents larger agglomerates. As the flame height is increased, N also increases due to fast coagulation and growth of smaller particles as stated before. Subsequently it achieves a maximum and then start decreasing again until flame heights close to the smoke point. This could be due to more intense oxidation at the tip of the flame for larger flames. After the smoke point N tends to increase again, due to the opening of the tip allowing for particles to pass through the flame. The $\langle dp \rangle$ as a function of flame height in this mode resembles the behaviour and trends of the overall PSD $\langle dp \rangle$.

It is clearly noted in all the results that the fuels substituted with larger aliphatic chains, such as PCH and BB, produce particles with smaller $\langle dp \rangle$. Alkylated aromatics cannot be presumed to have the same oxidation chemistry as those without side-chains, though some similarities should be expected. While some pathways produce identical products, others would yield species unique to the structure of the side chain. Alkylated aromatics, like their analogue alkanes will react by scission as the chain length increases and the strength in C-C bond decreases. As the length of the side chain increases, the abstraction

of benzylic H atoms will be less important given the large number of alkyl H atoms that can successfully compete. In general, they would decompose to form styrene, benzene and benzyl radicals in addition to the corresponding alkyl, alkenyl, alkane, alkene or other fragments depending on the side-chain nature [5].

4 Conclusions

The PSDs of soot formed by the non-premixed combustion of selected pure aromatic hydrocarbons were examined by probe sampling/differential mobility spectroscopy. The influence of fuel structure on the number of particles and the soot mean diameter at the tip of different flame heights was studied. The behaviour below and above the smoke point was investigated.

At very low flame heights, soot particles are being formed and large amounts of incepted particles are observed, followed by fast coagulation. For all fuels at these flame heights the values of mean particle diameter ($\langle dp \rangle$) were almost the same. Around the smoke point a deceleration in the particle growth is observed, due to the transition of the flame tip from a closed defined one to an open soot trail. At this transition, the sampling point (tip of the visible flame) corresponds to a point where some particles are being partially oxidised and emitted out of the flame. After the smoke point $\langle dp \rangle$ increases fast again.

Two groups of fuels were identified with respect of $\langle dp \rangle$ attained. Toluene and TMB produced the larger $\langle dp \rangle$, while BB and PCH the lowest. Below the smoke point tetralin, having the lowest smoke point (highest sooting propensity), achieved $\langle dp \rangle$ in the range of BB and PCH, but after the smoke point the $\langle dp \rangle$ was in-between the two groups of fuels. These results indicate that aromatic fuels substituted with larger aliphatic chains produce particles with smaller $\langle dp \rangle$.

5 Acknowledgments

M.B acknowledges financial support provided by the Administrative Department of Science, Technology and Innovation of Colombia. This work was supported by the Singapore National Research Foundation under its Campus for Research Excellence And Technological Enterprise (CREATE) programme.

References

[1] A. Abid, N. Heinz, E. Tolmachoff, D. Phares, C. Campbell, and H. Wang. On evolution of particle size distribution functions of incipient soot in premixed ethylene-oxygen-argon flames. *Combustion and Flame*, 154:775–788, 2008.

[2] H. Anderson, C. S. McEnally, and L. D. Pfefferle. Experimental study of naphthalene formation pathways in non-premixed methane flames doped with alkylbenzenes. *Proceedings of the Combustion Institute*, 28(2):2577 – 2583, 2000. ISSN 1540-7489. doi:http://dx.doi.org/10.1016/S0082-0784(00)80675-X.

[3] ASTM. Standard test method for smoke point of kerosine and aviation turbine fuel. *ASTM Standard D1322-08*, 1997.

[4] D. Bradley and A. G. Entwistle. Determination of the emissivity, for total eadition, of small diameter platinum-10 rhodium wires in the themperture range 600-1450^{o}c. *British Journal of Applied Physics*, 12:708 – 711, 2008.

[5] K. Brezinsky. The high-temperature oxidation of aromatic hydrocarbons. *Progress in Energy and Combustion Science*, 12(1):1 – 24, 1986. ISSN 0360-1285. doi:10.1016/0360-1285(86)90011-0.

[6] H. F. Calcote and D. M. Manos. Effect of molecular structure on incipient soot formation. *Combustion and Flame*, 49(1-3):289–304, 1983. doi:10.1016/0010-2180(83)90172-4.

[7] M. Colket, T. Edwards, S. Williams, N. Cernansky, D. L. Miller, F. Egolfopoulos, P. Linstedt, R. Seshadri, F. L. Dryer, C. K. Law, D. G. Friend, D. Lenhert, H. Pitsch, A. Sarofim, M. Smooke, and W. Tsang. Development of an experimental database and kinetic models for surrogate jet fuels. *45th AIAA Aerospace Sciences Meeting and Exhibit Proceedings*, pages 1–21, 2007. 45th AIAA Aerospace Sciences Meeting and Exhibit.

[8] V. A. Cundy, J. S. Morse, and D. W. Senser. Constant-tension thermocouple rake suitable for use in flame mode combustion studies. *Review of Scientific Instruments*, 57(6):1209–1210, 1986. doi:http://dx.doi.org/10.1063/1.1138631.

[9] F. Douce, N. Djebaïli-Chaumeix, C.-E. Paillard, C. Clinard, and J.-N. Rouzaud. Soot formation from heavy hydrocarbons behind reflected shock waves. *Proceedings of the Combustion Institute*, 28(2):2523 – 2529, 2000. ISSN 1540-7489. doi:10.1016/S0082-0784(00)80668-2.

[10] J. T. Farrell, N. Cernansky, F. Dryer, C. K. Law, D. G. Friend, C. Hergart, R. M. McDavid, A. K. Patel, C. J. Mueller, and H. Pitsch. Development of an experimental database and chemical kinetic models for surrogate diesel fuels. *SAE technical paper*, 2007-01-0201(2007-01-0201), 2007. doi:10.4271/2007-01-0201.

[11] M. Frenklach, D. W. Clary, W. C. Gardiner, and S. E. Stein. Effect of fuel structure on pathways to soot. *Symposium (International) on Combustion*, 21(1):1067–1076, 1988. ISSN 0082-0784. doi:10.1016/S0082-0784(88)80337-0. Twenty-First Symposium (International) on Combustion.

[12] I. Glassman. Soot formation in combustion processes. *Symposium (International) on Combustion*, 22(1):295 – 311, 1989. ISSN 0082-0784. doi:10.1016/S0082-0784(89)80036-0.

[13] A. Gomez, G. Sidebotham, and I. Glassman. Sooting behavior in temperature-controlled laminar diffusion flames. *Combustion and Flame*, 58(1):45–57, 1984. ISSN 0010-2180. doi:10.1016/0010-2180(84)90077-4.

[14] R. A. Hunt. Relation of smoke point to molecular structure. *Industrial and Engineering Chemistry*, 45(3):602–606, 1953.

[15] M. Kasper, K. Siegmann, and K. Sattler. Evaluation of an in situ sampling probe for its accuracy in determining particle size distributions from flames. *Journal of Aerosol Science*, 28(8):1569 – 1578, 1997. ISSN 0021-8502. doi:10.1016/S0021-8502(97)00031-1.

[16] M. Maricq. Size and charge of soot particles in rich premixed ethylene flames. *Combustion and Flame*, 137(3):340 – 350, 2004. ISSN 0010-2180. doi:10.1016/j.combustflame.2004.01.013.

[17] M. Maricq. Physical and chemical comparison of soot in hydrocarbon and biodiesel fuel diffusion flames: A study of model and commercial fuels. *Combustion and Flame*, 158(1):105–116, 2011. ISSN 0010-2180. doi:10.1016/j.combustflame.2010.07.022.

[18] M. Maricq. Soot formation in ethanol/gasoline fuel blend diffusion flames. *Combustion and Flame*, 159(1):170–180, 2012. ISSN 0010-2180. doi:10.1016/j.combustflame.2011.07.010.

[19] O. Mathieu, N. Djebaïli-Chaumeix, C.-E. Paillard, and F. Douce. Experimental study of soot formation from a diesel fuel surrogate in a shock tube. *Combustion and Flame*, 156(8):1576 – 1586, 2009. ISSN 0010-2180. doi:10.1016/j.combustflame.2009.05.002.

[20] C. S. McEnally, *Ü*mit *Ö*. K*ö*ylü, L. D. Pfefferle, and D. E. Rosner. Soot volume fraction and temperature measurements in laminar nonpremixed flames using thermocouples. *Combustion and Flame*, 109(4):701 – 720, 1997. ISSN 0010-2180. doi:http://dx.doi.org/10.1016/S0010-2180(97)00054-0.

[21] C. S. McEnally, L. D. Pfefferle, B. Atakan, and K. Kohse-H*ö*inghaus. Studies of aromatic hydrocarbon formation mechanisms in flames: Progress towards closing the fuel gap. *Progress in Energy and Combustion Science*, 32(3):247–294, 2006. ISSN 0360-1285. doi:10.1016/j.pecs.2005.11.003.

[22] A. Mouis, A. Menon, V. Katta, T. Litzinger, M. Linevsky, R. Santoro, S. Zeppieri, M. Colket, and W. Roquemore. Effects of m-xylene on aromatics and soot in laminar, n2-diluted ethylene co-flow diffusion flames from 1 to 5xa0;atm. *Combustion and Flame*, 159(10):3168 – 3178, 2012. ISSN 0010-2180. doi:http://dx.doi.org/10.1016/j.combustflame.2012.03.014.

[23] D. Olson, J. Pickens, and R. Gill. The effects of molecular structure on soot formation II. diffusion flames. *Combustion and Flame*, 62(1):43–60, 1985.

[24] W. Pitz, N. Cernansky, F. Dryer, F. Egolfopoulos, J. T. Farrell, D. G. Friend, and H. Pitsch. Development of an experimental database and chemical kinetic models for surrogate gasoline fuels. *SAE technical paper*, 2007-01-0175(2007-01-0175), 2007. doi:10.4271/2007-01-0175.

[25] M. Saffaripour, M. Kholghy, S. Dworkin, and M. Thomson. A numerical and experimental study of soot formation in a laminar coflow diffusion flame of a jet A-1 surrogate. *Proceedings of the Combustion Institute*, 34(1):1057–1065, 2013. ISSN 1540-7489. doi:10.1016/j.proci.2012.06.176.

[26] R. Schalla and G. McDonald. Variation in smoking tendency among hydrocarbons of low molecular weight. *Industrial and Chemical Chemistry*, 45(7):1497–1500, 1953.

[27] C. R. Shaddix. Correcting thermocouple measurements for radiation loss: a critical review. *Proceedings of 33rd National Heat Transfer Conference*, (HTD99-282), 1999.

[28] K. Siegmann, K. Sattler, and H. Siegmann. Clustering at high temperatures: carbon formation in combustion. *Journal of Electron Spectroscopy and Related Phenomena*, 126(1-3):191–202, 2002. ISSN 0368-2048. doi:10.1016/S0368-2048(02)00152-4.

[29] United Nations. Regulation no.83: Uniform provisions concerning the approval of vehicles with regard to the emission of pollutants according to engine fuel requirements, 2010.

[30] R. J. Watson, M. L. Botero, C. J. Ness, N. M. Morgan, and M. Kraft. An improved methodology for determining threshold sooting indices from smoke point lamps. *Fuel*, 111:120 – 130, 2013. ISSN 0016-2361. doi:10.1016/j.fuel.2013.04.024.

[31] B. Zhao, Z. Yang, M. Johnston, H. Wang, A. Wexler, M. Balthasar, and M. Kraft. Measurement and numerical simulation of soot particle size distribution functions in a laminar premixed ethylene-oxygen-argon flame. *Combusiton and Flame*, 133: 173–188, 2003.

[32] B. Zhao, Z. Yang, J. Wang, M. Johnston, and H. Wang. Analysis of soot nanoparticles in a laminar premixed ethylene flame by scanning mobility particle sizer. *Aerosol Science and Technology*, 37:611–620, 2003.